HEFAT2010
7th International Conference on Heat Transfer, Fluid Mechanics and Thermodynamics
19-21 July 2010
Antalya, Turkey

EXPERIMENTAL STUDY ON EVAPORATION CHARACTERISTICS OF UREA-WATER-SOLUTION DROPLETS FOR SCR APPLICATIONS

Seungyeol Lee* and Seungwook Baek
*Author for correspondence
School of Mechanical, Aerospace and Systems Engineering,
Korea Advanced Institute of Science and Technology(KAIST),
Daejeon,
Republic of Korea,
E-mail: naltl14@kaist.ac.kr

ABSTRACT

The evaporation behavior of urea-water-solution (UWS) droplet was investigated for application to urea-selective catalytic reduction (SCR) systems. A number of experiments were performed with single UWS droplet suspended on the tip of a fine quartz fiber. To cover the temperature range of real-world diesel exhausts, droplet ambient temperature was regulated from 373 to 873K using an electrical furnace. As a result of this study, UWS droplet revealed different evaporation characteristics depending on its ambient temperature. At high temperatures, it showed quite complicated behaviors such as bubble formation, distortion, and partial rupture after a linear D^2-law period. However, as temperature decreases, these phenomena became weak and finally disappeared. Also, droplet diminishment coefficients were extracted from transient evaporation histories for various ambient temperatures, which yields a quantitative evaluation on evaporation characteristics of UWS droplet as well as provides valuable empirical data required for modeling or simulation works on urea-SCR systems.

INTRODUCTION

Among various techniques of SCR, the most realistic solution capable of reducing diesel NOx to levels required by stringent worldwide emission standards is ammonia-selective catalytic reduction (SCR) which uses ammonia as a reducing agent[1]. However, due to inherent toxicity and handling problems with pure ammonia, aqueous urea solution is now practically utilized as an alternative to the direct use of ammonia for mobile SCR applications.

Once urea-water-solution (UWS) spray is injected into hot exhaust gas stream before SCR catalyst, water content first evaporates from UWS. Then, ammonia is generated in-situ through both thermal decomposition of urea and hydrolysis of isocyanic acid as follows [2-4].

$$(NH_2)_2CO \rightarrow NH_3 + HNCO \quad (1)$$

$$HNCO + H_2O \rightarrow NH_3 + CO_2 \quad (2)$$

By collectively reviewing the literatures [5-8], it is found that the state of aggregation urea is not clear during the evaporation of UWS, rather it can be varied among solid, molten, and gas phases depending on thermo-physical conditions.

After that, ammonia produced by the above reactions (1) and (2) takes part in various deNOx reactions as a reductant. Main deNOx reactions under a typical diesel exhaust environment can be summarized as follows [5,9].

$$4NH_3 + 4NO + O_2 \rightarrow 4N_2 + 6H_2O \quad (3)$$

$$4NH_3 + 2NO + 2NO_2 \rightarrow 4N_2 + 6H_2O \quad (4)$$

$$4NH_3 + 3NO_2 \rightarrow 7/2\, N_2 + 6H_2O \quad (5)$$

$$4NH_3 + 4NO + 3O_2 \rightarrow 4N_2O + 6H_2O \quad (6)$$

However, in urea-SCR systems, several negative effects are possibly derived due to the use of UWS. Sullivan and Doherty[10], on the basis of experiments with several oxide-supported copper catalysts, proposed a possibility that urea does not hydrolyze according to reactions (1) and (2) and instead it reacts with O_2 to form N_2 fruitlessly as follows.

$$(NH_2)_2CO + O_2 \rightarrow CO_2 + H_2O + N_2 \quad (7)$$

Moreover, deposit formation is a highly critical problem. Various urea decomposition products (i.e., biuret, cyanuric acid (CYA), ammelide, ammeline, melamine, etc.) and their polymeric complexes involving hydrogen bondings can be generated in urea-SCR systems. Fang and DaCosta [8] reported that urea thermolysis involves two decomposition stages; one is ammonia generation stage which is desirable for reducing NOx, whereas the other is ammonia consumption stage which promotes the formation of undesirable species. In particular, consecutive decompositions after ammonia consumption stage lead to the production of melamine complexes which are

considered as a major source to hinder the performance of catalyst by not only consuming a part of ammonia produced during urea thermolysis but also degrading the structural and thermal properties of catalyst surface.

A sufficient understanding on the behavior of UWS spray is prerequisite for controlling the formation of urea-derived deposits. However, there are lots of complexities involved in the evaporation process of UWS at a heated environment. Dissolved urea influences the evaporation of water from UWS and simultaneously urea itself undergoes thermal decomposition as well as reacts to produce various species. Because of these difficulties, the evaporation behavior of UWS has not been clearly understood yet.

In this study, the evaporation behavior of UWS droplet was experimentally observed over the temperature range of actual diesel exhaust. Measurements were conducted by changing droplet ambient temperature by 50K from 373 to 873K. Main objectives of this study are to understand the evaporation characteristics of UWS droplet in various ambient temperatures and also to provide empirical evaporation coefficients which can be utilized as reference data in modeling or simulation works on UWS spray. So far, to our knowledge, there have been few useful experimental data capable of quantifying the evaporation of UWS droplet over a wide range of temperatures.

EXPERIMENTS

Procedures and facilities

In this study, AdBlue (contains 32.5% urea by weight) is used as a representative UWS. A schematic view of experimental setup is illustrated in Figure 1. In this section, experimental procedures and facilities are described and further details can be found in Ghassemi et al. [10,11].

First, an electrical furnace is lifted up away from a droplet suspension system and its interior temperature is regulated to an intended value using controller and thermocouple. Once the control of droplet ambient temperature is completed, then single UWS droplet is suspended around a bead that is placed at the tip of a quartz fiber (diameter=0.125mm) using a droplet maker whose end part is equipped with a hollow stainless-steel needle (outer diameter=0.21mm). The movement of this droplet maker is adjusted by handling a lever, which causes liquid UWS to transport to the bead, thereby generating a droplet.

The next step is to drop electrical furnace to the position as shown in dotted line in Figure 1. Then, this leads the suspended UWS droplet to be exposed to high temperature, which eventually yields its evaporation. Glass window enables us to observe the evaporation process of droplet using a high-speed charge-coupled device (CCD) camera and its pictured images are recorded on a computer.

It should be noted that there are several error sources in measuring the evaporation rate of UWS droplet under a constant temperature condition. Despite these errors, a certain degree of measurement accuracy may be conserved in this study. By virtue of self-controlling temperature system as well as rapid increase in temperature using electrical heating element, it is possible to sustain the ambient temperature of droplet to a nearly constant value without significant variation. In addition, conduction heat transfer between fiber and droplet is almost negligible because the thickness of quartz suspension fiber is very thin. Radiation heat transfer from heating element coils placed at furnace inner walls to droplet is also minimized using radiative shields equipped around the coils.

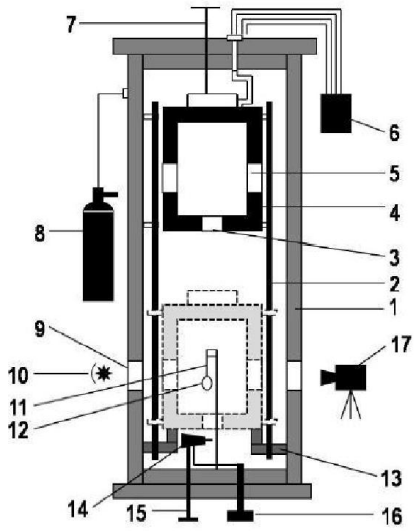

Figure 1 A schematic view of experimental setup

1: cylindrical vessel, 2: guide bar, 3: furnace bottom hole, 4: electric furnace, 5: quartz glass window on furnace, 6: temperature controller, 7: furnace lever, 8: air vessel, 9: quartz glass window on pressure vessel, 10: backlight source, 11: quartz fiber, 12: droplet, 13: shock absorber, 14: droplet maker, 15: droplet lever, 16: plunger micro-pump, 17: high-speed CCD camera.

Extracting droplet diameter and evaporation coefficient

Figure 2 shows a sample of image of UWS droplet that was captured during evaporation. Here, the needle beside droplet-suspended fiber provides a reference scale of known diameter (0.21mm). To extract droplet diameter from the picture, a flexible image-processing program was developed using Visual Basic language. In this program, the number of pixels corresponding to the diameter of reference needle is first calculated. Then, an imaginary square of known area is drawn around droplet as shown in Figure 2. After that, the number of pixels that constitute droplet is calculated on the basis of intensity difference from surroundings. Finally, the area of a concentric circle having the same number of pixels is calculated, which in turns gives droplet diameter from the law of proportion with reference needle. This procedure is executed iteratively for each image file, which yields a temporal variation of droplet diameter during evaporation.

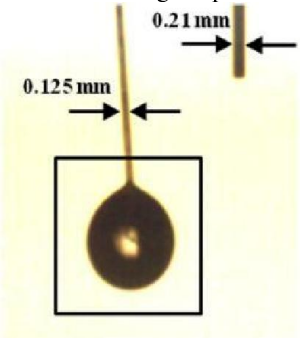

Figure 2 A sample photograph of evaporating UWS droplet

In general, the early lifetime of evaporating droplet shows a nonlinear behavior due to transient droplet heat-up from environment and subsequent thermal expansion. As droplet temperature increases, a balance between thermal expansion and evaporation determines the size of droplet at that time. Once the temperature inside droplet reaches a quasi-steady state, only evaporation becomes effective in determination of the size of droplet. Starting from this stage, an evaporation process according to the D^2-law of droplet becomes valid. Regarding the linear D^2-law part, droplet evaporation is quantitatively characterized by the following evaporation coefficient, K.

$$K = \frac{d\left(D^2\right)}{dt} \tag{8}$$

This droplet evaporation coefficient is extracted from the temporal history of squared droplet diameter by measuring the slope of its linear regression part. In this study, the above procedure is also used to obtain the evaporation coefficient of UWS droplet.

RESULTS AND DISCUSSION

Evaporation characteristics of UWS droplet with ambient temperature

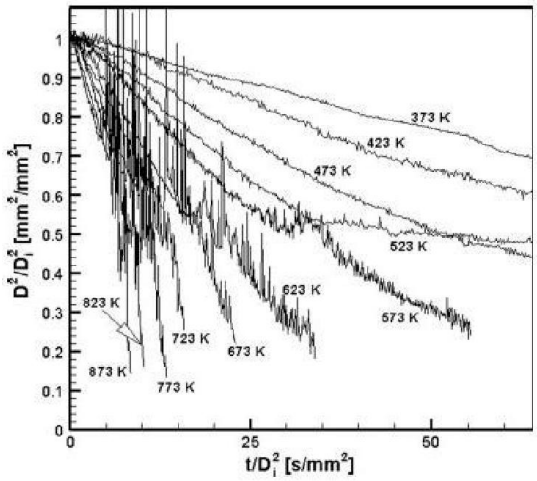

Figure 3 Normalized temporal variations of the diameter squared of evaporating UWS droplets with ambient temperature

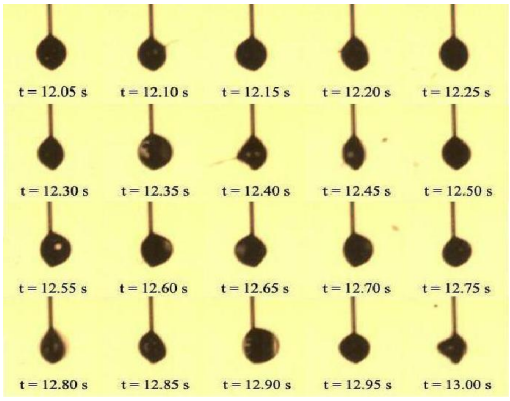

Figure 4 Sequential photographs of evaporating UWS droplet at 773 K which show microexplosion.

Figure 3 shows normalized temporal variations of the diameter squared of UWS droplets evaporating at ambient temperatures from 373 to 873K. Note that, to minimize initial droplet size effect on its evaporation, experiments were performed with the droplets having similar initial diameters (from 0.758 to 0.963mm). As shown in the figure, UWS droplets displayed different evaporation behaviors depending on their ambient temperature. From this observation, the evaporation characteristics of UWS droplet can be classified into several groups according to the range of ambient temperature.

Also, Figure 3 reveals that droplet microexplosion begins to appear at 573K and it becomes more intense with increase in ambient temperature. Figure 4 presents sequential photographs of evaporating UWS droplet at 773K and microexplosion phenomenon is clearly observed here. Droplet internal bubble formation appears from the because of its rapid expansion. Also, droplet distortion is seen from the photos and droplet fragmentation is shown. Note that these irregular behaviors are typically observed in the evaporation process of multicomponent droplet [10].

For ambient temperatures of 373 and 423K

As shown in Figure 3, UWS droplets evaporating at both 373 and 423K exhibit almost linear history. The whole lifetime of each droplet is presented in Figure 5.

The melting point of urea is known to 406±3K [12]. Therefore, at ambient temperature of 373 K, only water content will evaporate from UWS droplet. On the other hand, at 423K, urea near droplet surface is expected to melt and thermally decomposes into ammonia and isocyanic acid according to reaction (1). However, as shown in Figure 5, the current experimental result at 423K exhibits a similar evaporation behavior to that of 373K. Hence, urea gasification was not clearly observed at 423K in this study. This observation is consistent with the result produced by Schaber et al. [7] who reported that a vigorous gas evolution from molten urea commences at 425K.

To estimate the evaporation coefficient of UWS droplet, the least square regression method was used with the data corresponding to linear part of evaporation history except both initial heat-up and final solidification periods. The estimated evaporation coefficients were given with actual measurement data in Figure 5.

The deposits produced at these ambient temperatures may be composed only of solidified urea because the first urea-derived species, biuret, begins to be generated from the reaction of isocyanic acid with intact urea at ~433K [7]. Sequential photographs including evaporation and solidification processes of UWS droplet at 373K are displayed in Figure 6, and therein observations after 75s indicate that deposit undergoes no change. At 373K, UWS droplet shows solid-like behavior because dissolved urea is never melted at this ambient temperature during the whole evaporation period. On the other hand, at 423K, UWS droplet exhibits more liquid-like characteristic because dissolved urea is possibly heated over its melting point and, therefore, exists as a molten state at this temperature.

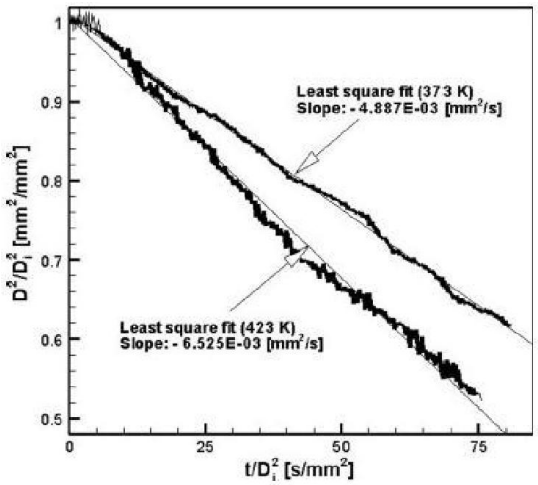

Figure 5 Normalized temporal variations of the diameter squared of evaporating UWS droplets with the least square fit to linear water evaporation part (bold solid fine) at both 373 K and 423 K

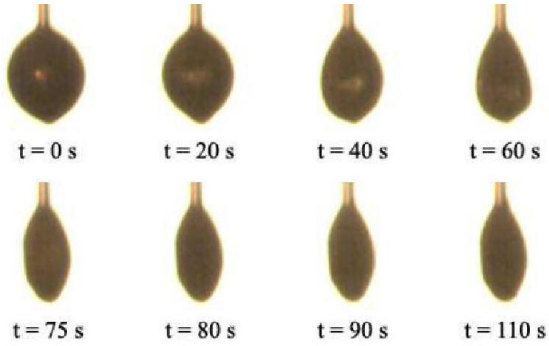

Figure 6 Sequential photographs of evaporating UWS droplet at 373 K

For ambient temperatures of 473 and 523K

Figure 7 displays normalized temporal variations of the diameter squared of evaporating UWS droplets at both 473 and 523K. Evaporation histories at these ambient temperatures can be divided into two distinguished stages because of the obvious difference in their diminishing rates. During the first-stage evaporation period, it is expected that water content mainly evaporates from UWS droplets. Musa et al. [13] compared the evaporation behavior of UWS droplet with distilled water and therein almost no difference in their first-stage evaporation was observed. On the other hand, during the second-stage evaporation, the gasification of urea may be a dominant mechanism responsible for diminishment in UWS droplet size.

Previously, at temperatures of 373 and 423K, urea gasification did not appear to occur. However, at 473 and 523K, it was clearly observed after the complete depletion of liquid component. Perhaps, this is because the decomposition of urea rapidly enhances above 425K [7]. Therefore, at temperatures of 473 and 523K, the diminishment rate of UWS droplet should be determined respectively for both stages to completely quantify its entire evaporation period. Here, the least square method was also utilized to find the slope of each stage. A comparison of two evaporation histories presented in Figure 7 indicates that the difference in the slope of each stage becomes smaller with increase in ambient temperature. Figure 8 displays sequential photographs of evaporating UWS droplet at 473K .

Also, at these temperatures, solidified deposit was observed to remain finally as in the previous case of 373 and 423K. However, its constituents may be different. Referring to the pyrolysis experiment conducted by Schaber et al. [7], the deposits generated at 473 and 523K probably consist of several urea-derived products such as biuret, CYA, ammelide, and ammiline with the undecomposed urea itself.

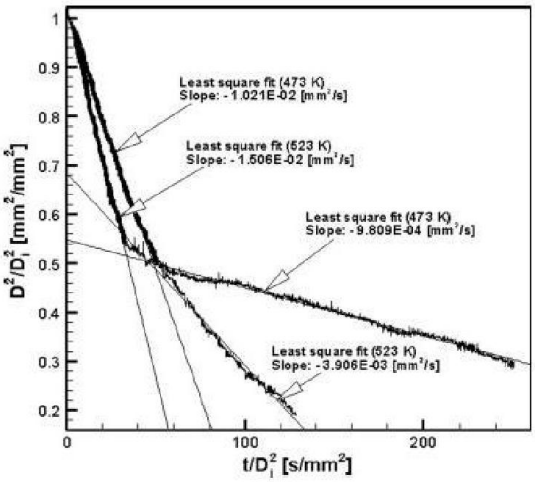

Figure 7 Normalized temporal variations of the diameter squared of evaporating UWS droplets with the least square fit to linear water evaporation part (bold solid fine) at both 473 K and 523 K

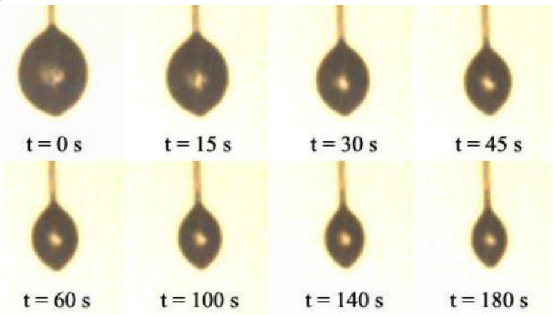

Figure 8 Sequential photographs of evaporating UWS droplet at 473 K

For ambient temperatures of 573 and 623K

Figure 9 shows normalized evaporation histories at both 573 and 623K. The most distinguished feature of evaporating UWS droplets at these ambient temperatures is the onset of microexplosion. In Figure 9, after the first linear evaporation period, droplet re-expansion is observed with a fluctuating behavior. The reason for this fluctuation is that more volatile component trapped inside UWS droplet due to diffusional resistance is heated beyond local boiling point, which causes homogeneous nucleation and thereby droplet internal pressure build-up. Here, the rates of both nucleation and diffusion compete against each other, whose difference influences droplet expansion characteristics. A comparison of two evaporation histories reveals that more intense fluctuation

occurs at higher temperature. A fast internal pressure build-up caused by rapid nucleation at higher temperature results in more aggressive evaporation behaviors.

To obtain the evaporation coefficient of the first stage, the least square method was also applied to the linear part of experimental data. However, for the next evaporation stage, the use of the least square method is not justified due to droplet expansion and fluctuation so that its diminishment rate is simply estimated using the slope determined with two end points. Note that, from the comparison of two evaporation histories, the difference in diminishment rates of both the first and the second stages becomes smaller as ambient temperature increases.

Sequential photographs of the whole evaporation process at 573K are displayed in Figure 10. At temperatures of 573 and 623K, solidified deposits were also observed to remain after the complete depletion of liquid component. However, their amount is much smaller when compared with the previous lower-temperature cases. It should be noted that these deposits may be composed of the same constituents as those of 473 and 523K.

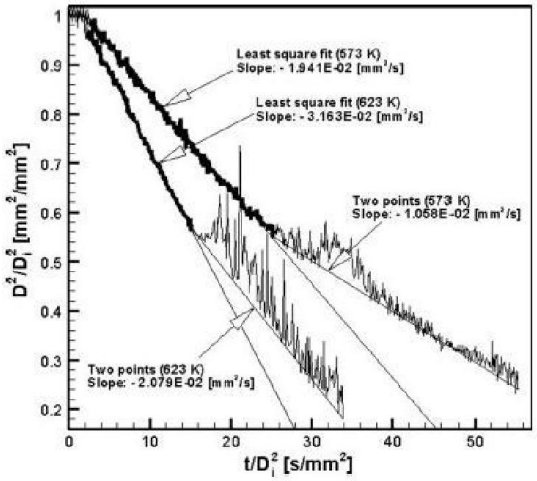

Figure 9 Normalized temporal variations of the diameter squared of evaporating UWS droplets with the least square fit to linear water evaporation part (bold solid line) and two-point estimation to urea gasification part (thin solid line) at both 573 K and 623 K

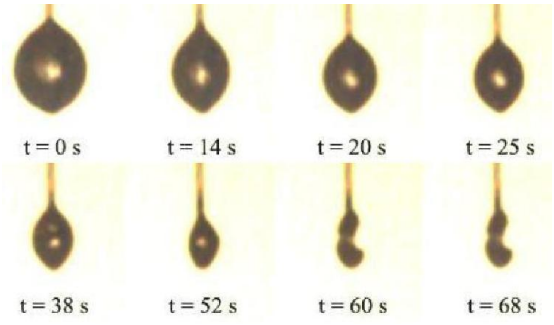

Figure 10 Sequential photographs of evaporating UWS droplet at 573 K

For ambient temperatures of 673 and 723K

Figure 11 illustrates normalized evaporation histories of UWS droplets at 673 and 723K. In this experiment, there was almost no difference in evaporation characteristics at ambient temperatures above 673K. Hence, evaporation histories obtained over 673K showed the same profile as displayed in Figure 11 except for the magnitude of their slope. The diminishment rates of both the first and the second stages were increased with ambient temperature. Particularly in these temperatures of 673 and 723K, the magnitude of the first-stage evaporation rate is almost equal to that of the second-stage rate as can be seen from both evaporation histories in Figure 11.

Photographs of solidified deposits remaining after the complete depletion of liquid component at temperatures from 623 to 823K are displayed in Figure 12. As shown in the pictures, the amount of deposit remained was considerably reduced as ambient temperature rises from 623 to 673K. This may be attributed that the decomposition of CYA is completed between 648 and 653K as well as the sublimation and decomposition of ammelide occurs significantly at temperatures from 623 to 673K.

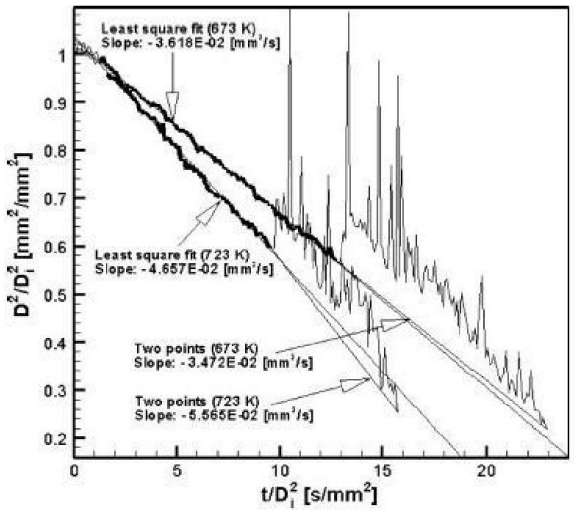

Figure 11 Normalized temporal variations of the diameter squared of evaporating UWS droplets with the least square fit to linear water evaporation part (bold solid line) and two-point estimation to urea gasification part (thin solid line) at both 673 K and 723 K

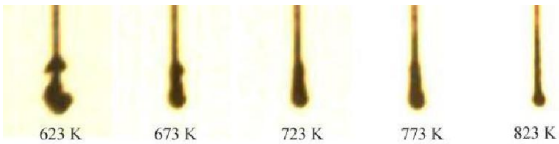

Figure 12 Photographs of solidified deposits remaining after the complete evaporation of UWS droplets for various ambient temperatures

For ambient temperatures of 773, 823 and 873K

Figure 13 presents normalized evaporation histories of UWS droplets at 773–873K. In this temperature range, the second-stage diminishment rate becomes faster than the first-stage rate. This is primarily because droplet microexplosion occurs more aggressively when compared with the case of 673 and 723K; Figures 13 reveals more intense second-stage evaporation behaviors than Figure 11. Note that the difference

in diminishment rates of both the first and the second stages becomes larger as ambient temperature rises from 773 to 873K.

In this experiment, solidified deposits were still observed to remain up to 773K, while almost no deposit was found for ambient temperatures of 823 and 873K. It is known that ammelide is completely eliminated at about 873K, while ammeline requires temperatures over 973K [7]. Therefore, it can be deduced that quite a tiny amount of ammeline is produced during the evaporation of UWS droplet. If ammeline was produced considerably, then a certain amount of deposit would be observed even at temperatures exceeding 823K. Also, it is known that CYA is completely disappeared below 673K. As a consequence, the deposits remaining at temperatures from 673 to 773K are mainly composed of ammelide.

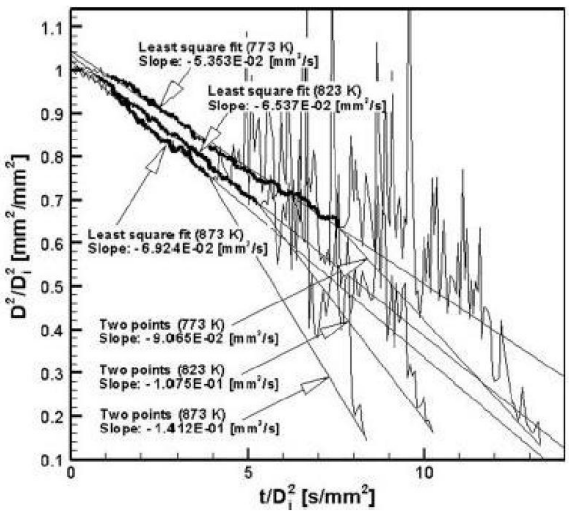

Figure 13 Normalized temporal variations of the diameter squared of evaporating UWS droplets with the least square fit to linear water evaporation part (bold solid line) and twopoint estimation to urea gasification part (thin solid line) at 773 K, 823 K, and 873 K

CONCLUSIONS

In this study, the evaporation behavior of UWS droplet was investigated using suspended droplet experiment. Through a number of repeated measurements, evaporation rates were extracted for a variety of initial droplet diameters and ambient temperatures. As a consequence, the current study helps to understand the evaporation characteristic of UWS droplet quantitatively as well as qualitatively. Furthermore, this study provides some empirical data required in modeling or simulation works on urea-SCR system. A summary of the results is as follows.

(1) On the basis of the current observations, the evaporation behavior of UWS droplet can be categorized into several groups according to ambient temperature. At 373 and 423K, UWS droplet evaporates without being divided into two stages. At 473 and 523K, both evaporation periods of the first and second stages commonly show linear diminishment, while they are obviously distinguished by the difference in their rates. At 573 and 623K, weak microexplosion appears and the first-stage rate exceeds the second-stage rate. At 673 and 723K, strong microexplosion appears and the first-stage rate almost equals the second-stage rate. At 773 to 873K, very strong microexplosion appears and second-stage rate exceeds the first-stage rate.

(2) After the complete depletion of liquid component constituting UWS droplet, solidified deposit is observed to remain at temperatures below 773K and its amount is reduced with increase in ambient temperature, while there is almost no deposit remained at temperatures above 823K.

ACKNOWLEDGMENTS

This work was supported by the Korea Science and Engineering Foundation (KOSEF) grant funded by the Korea government (MEST) (No.2009-0079086)

REFERENCES

[1] http://www.DieselNet.com, Selective Catalytic Reduction, In: Diesel-Net Technology Guide, 2002.

[2] Koebel M, Elsener M. Determination of urea and its thermal decomposition products by high-performance liquid chromatography. *J Chromatogr A*. 1995;689:164–169.

[3] Yim SD, Kim SJ, Baik JH, Nam IS, Mok YS, Lee JH, Cho BK, Oh SH. Decomposition of urea into NH_3 for the SCR process. I*nd Eng Chem Res.* 2004;43:4856–4863.

[4] Kleemann M, Elsener M, Koebel M, Wokaun A. Hydrolysis of isocyanic acid on SCR catalysts. *Ind Eng Chem Res*. 2000;39:4120–4126.

[5] Koebel M, Elsener M, Kleemann M. Urea-SCR: a promising technique to reduce NOx emissions from automotive diesel engines. *Catal Today*. 2000;59:335–345.

[6] Koebel M, Elsener M, Marti T. NOx-reduction in diesel exhaust gas with urea and selective catalytic reduction. *Combust Sci Tech.* 1996;121:85–102.

[7] Schaber PM, Colson J, Higgins S, Thielen D, Anspach B, Brauer J. Thermal decomposition (pyrolysis) of urea in an open reaction vessel. *Thermochim Acta*. 2004;424:131–142.

[8] Fang HL, DaCosta HFM. Urea thermolysis and NOx reduction with and without SCR catalysts. *Appl Catal B: Environ.* 2003;46: 17–34.

[9] Koebel M, Elsener M, Madia G. Reaction pathways in the selective catalytic reduction process with NO and NO_2 at low temperatures. *Ind Eng Chem Res.* 2001;40:52–59.

[10] Ghassemi H, Baek SW, Khan QS. Experimental study on binary droplet evaporation at elevated pressures and temperatures. *Combust Sci Tech*. 2006;178:1031–1053.

[11] Ghassemi H, Baek SW, Khan QS. Experimental study on evaporation of kerosene droplets at elevated pressures and temperatures. *Combust Sci Tech.* 2006;178:1669–1684.

[12] http://webbook.nist.gov/chemistry/,NIST Chemistry WebBook, NIST Standard Reference Database No. 69, 2005.

[13] Musa SNA, Saito M, Furuhata T, Arai M. Evaporation characteristics of a single aqueous urea solution droplet. *ICLASS-2006, Kyoto, Paper ID ICLASS06-195,* 2006.